Peer-reviewed version available at Drones 2019, 3, 6; doi:10.3390/drones3010006

Research Article

Greenness indices from a low-cost UAV imagery as tools for monitoring after-fire forest recovery

Asier R. Larrinaga[1,2,3]* and Lluís Brotons[1,4,5]

[1] InForest Joint Research Unit, (CTFC-CREAF) Solsona 25280, Spain. lluis.brotons@ctfc.cat
[2] eNeBaDa, Santiago de Compostela, 15892, A Coruña, Spain. asier@enebada.eu
[3] Forest Genetics and Ecology Group, Biologic Mission of Galicia (CSIC), Pontevedra 36413, Spain. arodriguez@mbg.csic.es
[4] CREAF, Cerdanyola del Vallès 08193, Spain
[5] CSIC, Cerdanyola del Vallès 08193, Spain
* Correspondence: asier@enebada.eu; Tel.: +34-659-087889

Abstract: During recent years UAVs have been increasingly used in agriculture and forestry research and application. Nevertheless, most of this work has been devoted to improving accuracy and explanatory power, often at the cost of usability and affordability. We tested a low-cost UAV and a simple workflow to apply four different greenness indices to the monitoring of pine (*Pinus sylvestris* and *P. nigra*) after-fire regeneration in a Mediterranean forest. We selected two sites and masured all pines within a pre-selected plot. Winter flights were carried out at each of the sites, at two flight altitudes (50 and 100 m). Automatically normalizing images entered an SfM based photogrammetric software for restitution and the obtained point cloud and orthomosaic processed to get a canopy height model and four different greenness indices. Sum of pine DBH was regressed on summary statistics of greenness indices and canopy height model. ExGI and GCC indices outperformed VARI and GRVI in estimating pine DBH, while canopy height model slightly improved the models. Flight altitude did not severely affect model performance. Our results show that low cost UAVs may improve forest monitoring after disturbance, even in those habitats and situations were resource limitation is an issue.

Keywords: low-cost UAV; greenness index; *Pinus nigra*; *Pinus sylvestris;* forest regeneration; flight altitude; small UAV

1. Introduction

During recent years, UAVs (unmanned aerial vehicles) have grown increasingly popular for the study of land and its cover (Hardy & Hardy 2010, Colomina & Molina 2014). This trend is the consequence of a recent exponential development of both the UAV industry and the DIY community, fostered by the technological advances in robotics and the miniaturization of electronics.

Forest research is one of the fields where the use of UAV has promised immediate benefits (Hardy & Hardy 2010). UAVs allow reducing the costs of airborne photography and LIDAR and approaches technology to its final user (Colomina & Molina 2014, Matese et al. 2015). By doing so, it offers a great flexibility. UAV deployment is fast and cheap, ensuring rapid responses to the needs of the academy and the industry and allowing for repeated sampling with no limits on deployment periodicity. A new, tailor-cut telemetry sampling strategy is now possible, designed to fit the specific needs of each case study (Matese et al. 2015).

UAVs have been used to discriminate among species and provide estimates of tree and stand size, tree cover, canopy height, gap abundance or even productivity, alone or in combination with LIDAR data (Wallace et al. 2012, Getzin et al. 2014, Salamí et al. 2014, Díaz-Varela et al. 2015, Puliti et al. 2015, Guerra-Hernández et al. 2016, Kaerpina et al. 2016, Baena et al. 2017, Thiel & Schmullius

2017). Tree health and pathogen or parasite attack have also been evaluated by means of UAV telemetry (Nebiker et al. 2008).

Therefore, research on different methodologies and, more specifically, on the accuracy of those data estimated by means of UAV imagery has bloomed during the last five years (Colomina & Molina 2014). The accuracy level of these kind of works is continuously increasing and it is a major focus of an important body of research on UAV use in forestry (Wallace et al. 2012, Colomina & Molina 2014, Puliti et al. 2015, Wallace et al. 2016, Gianetti et al. 2018, Puliti et al. 2018). Spatial accuracy and automatic tree detection in particular are rapidly improving (Blaschke 2010, Chehata et al. 2011, Torres-Sánchez et al. 2015, Guerra-Hernández et al. 2016, Thiel & Schmullius 2017, Puliti et al. 2018).

Nevertheless, accuracy is not always the main constraint to UAV use in forestry science. In fact, pursuing high standards of spatial and analytical accuracy is a time consuming goal that often requires an important investment. While this might be a sensible approach when working with economically exploited forests and woodlands, it might hinder the development of forestry research in other areas or research fields, such as disturbance response, where immediate revenues cannot be envisaged. In these situations, the absence of any kind of data is common and economic resources and work force scarce. A reduction of both accuracy and cost of deployment could hence help to get general data on the ecology of the forest that would greatly improve the knowledge.

In this work we explore the use of a low-cost UAV platform as a tool for monitoring recovery after a strong disturbance in a Mediterranean forest. Our objective is to assess post fire pine regeneration (Scots pine, *Pinus sylvestris*, and black pine, *P. nigra*) in an area affected by a wild fire in which oak has become the dominant tree species. In order to identify pine cover in our area, we compare the use of four different greenness indices at two different flight heights, a key determinant of accuracy, recorded area and hence cost. In this context, we aimed to develop a tool to monitor the emergence of pines that grow among the oaks and test the suitability of low-cost UAVs as a cost effective monitoring tool.

2. Materials and Methods

We carried out our work in the municipality of Riner, in the Lleida province, where an extensive wildfire burnt down around 25.000 ha of pine-dominated woodland in 1998. Most of the area have apparently recovered to a great extent in these last 18 years. A closer look, however, depicts a different picture. The effect of wildfire might have drawn the forest beyond its resilience threshold, causing a change to a new alternative equilibrium state (Rodrigo et al. 2004). In fact, although tree cover seems to be almost completely recovered, its species composition has changed in a radical way, as Portuguese oak (*Quercus faginea*) thrives in the burnt land where pines (*P. nigra* and *P. sylvestris*) were dominant before the wildfire.

Our two sites, La Carral and Cal Rovira-Sanca, in the municipality of Riner in the Lleida province (Catalonia, Spain). They are 3.7 km away from each other and both of them supported similar Mediterranean forests before the 1998 fire, on marl, limestone and sandstone rocks (Institut Cartogràfic i Geològic de Catalunya 2014).

2.1. UAV deployment and field sampling

We carried out two flight in each of the sites, one at a height of 50 m and a second one at a height of 100 m, by means of a DJI Phantom 2 quadcopter. The copter was equipped with a Phantom Vision FC200 camera, manufactured by DJI, which has a resolution of 14 Mpx with a sensor size of 1/2.3'' (6.17 mm * 4.55 mm) and a focal length of 5 mm. We set the camera to shot one picture every two seconds with an automatic exposition mode setting (with ISO 100).

All four flights were carried out on March 7 2015 (17 years after the fire) under optimal weather conditions; in Cal Rovira-Sanca in the morning and in the afternoon in La Carral. By flying in winter, we ensured a good spectral discrimination between pines –the only perennial tree species group in the area– and the remaining components of the canopy, namely Portuguese oaks –which still hold their dry leaves on the branches and do not shed new leaves until spring–.

In each of the sites we selected a sampling area within the flight area and identified all the pines within a preselected area located at the center of each sampling area (figure 1). Each pine was identified to the species level, located in a map and its height and diameter at breast height measured (DBH measured at 1m height).

Figure 1. Aerial ortophotographies of both sites, with overlapped positions of all the pines found in the sampling areas.

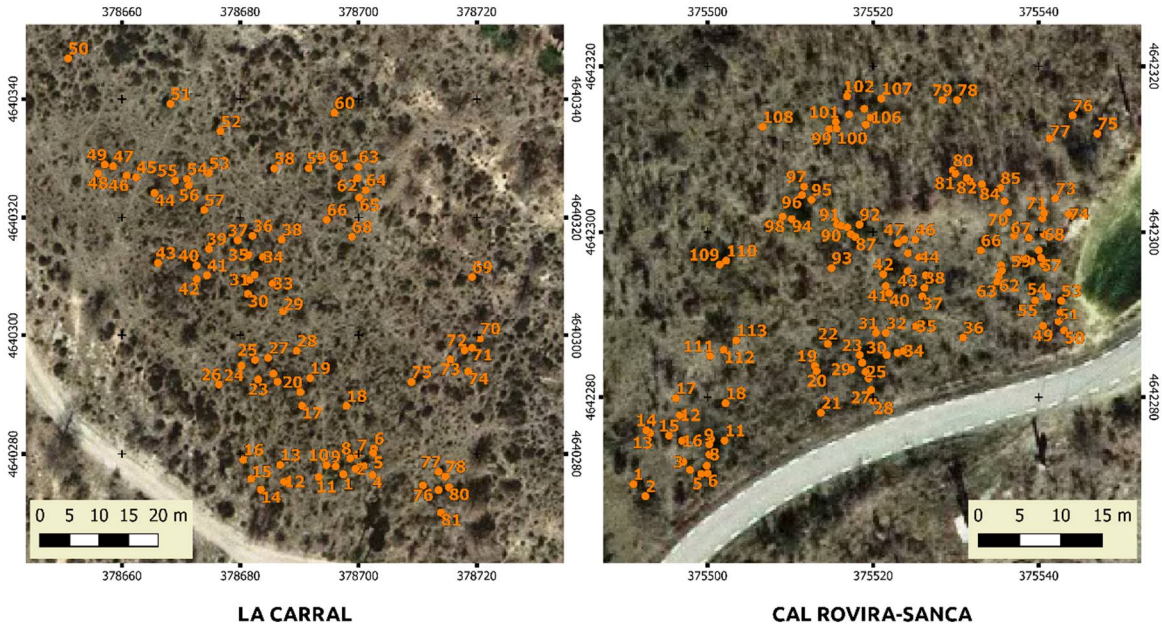

2.2. Image analysis

We aimed to get an easy workflow, and to that end, we tried to minimize parameter tweaking during the whole process. Hence, most of the procedures were carried out using automatic tools and algorithms, as well as default values for the various parameters. For the rest of the section, we will be giving details on the parameters we set specifically, while omitting those parameters that were set to their default values.

First we adjusted all the aerial images with XnViewMP (XnView MP 2016), by sequentially applying the Automatic Levels and Automatic Contrast tools. By doing so we corrected some inequalities in colour balance produced by the FC200 camera and improved their contrast for further analysis.

We followed the recommended workflow within Photoscan. Agisoft Photoscan is an advanced terrain-oriented software that can create 3D models, point clouds and orthomosaics from a set of images on the same subject, by means of SFM (structure from motion) techniques (Agisoft Photoscan Professional 2016; Westoby et al. 2012, Wallace et al. 2016). Photo aligning and estimation of camera locations and calibration parameters is carried out as a first step, together with the building of a sparse point cloud (figure 2). This sparse point cloud was then used to create a dense point cloud with mean point density of 407 points/m for the 50 m high flights and 69 points/m for the 100 m high flights. Finally, a digital elevation model and an orthomosaic were built from this point cloud, using the corresponding default tools in Photoscan.

Figure 2. General workflow for the analysis of UAV imagery, as shown by its intermediate output images, point clouds and 3D models. A detailed workflow is provided as Figure S2-1.

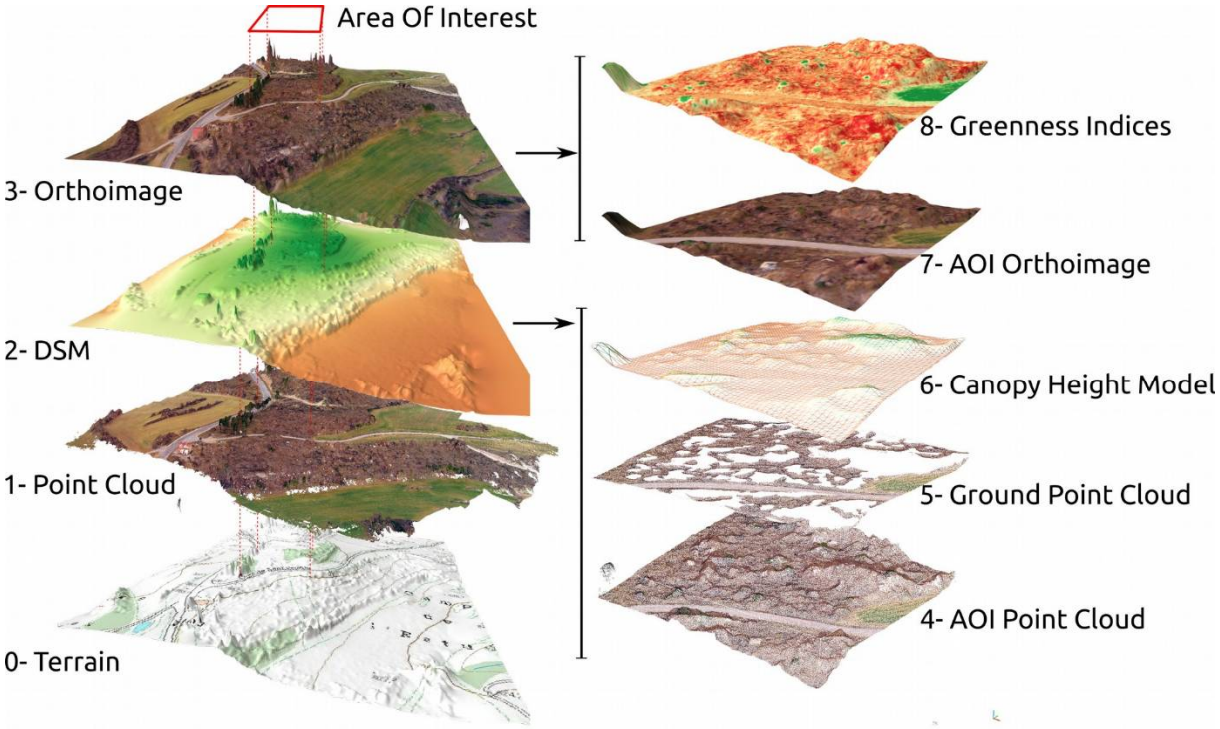

As a reference image to set control points, we used the most recent orthophoto of the area from the National Plan of Aerial Orthophography (Plan Nacional de Ortofotografía Aerea, PNOA), which has a pixel resolution of 25 cm. We set between 7 and 9 control points per flight by selecting particular features that could be identified both in the orthomosaic obtained from the Photoscan and in our reference aerial photography, such as stones, rocks, fallen trunks and artificial features (corners, road paint, etc.). We then used those control points to reconfigure the cameras and rebuild the dense point cloud, the DEM and the orthomosaic.

All the process within Photoscan was carried out with by-default parameters and pixel size was only set during the export step. We exported 50 m high flight orthomosaics and DEM with a pixel size of 2 and 8 cm, respectively, and those from 100 m high flights with pixels of 4 and 16 cm.

The obtained point cloud was then clipped by means of Fusion tools for forest LIDAR data analysis (McGaughey 2016), tool Clip). Misplaced points were detected in those clipped point clouds obtained from 50 m high flights and hence, they were cleaned up with CloudCompare, a point cloud editing and registering open software (CloudCompare 2016). Those from both 100 m high flights did not need such a cleaning process. We extracted those points corresponding to the ground level, by means of a filtering algorithm adapted from Kraus and Pfeifer (1998) as implemented in Fusion tools (tool GroundFilter), and then computed a digital terrain model (DTM) by using the mean elevation of all ground points within a cell (Fusion tools GridSurfaceCreate). From the highest elevation point in each cell and the created DEM, we built a canopy height model (Fusion tool CanopyModel) with a cell size of 10*10 cm2.

We calculated four different greenness indices from the obtained orthomosaic: excess green index (ExGI), green chromatic coordinate (GCC), green-red vegetation index (GRVI) and visible atmospherically resistant index (VARI):

* The excess green index (ExGI) is a contrast index that has been shown to outperform other indices in discriminating vegetation (Woebbecke et al. 1995, Sonnentag et al. 2012), and is defined as:

$$ExGI = 2 * G - (R + B) \quad \text{[eq. 1]}$$

* The green chromatic coordinate has also been used to detect vegetation and analyses plant phenology and dynamics (Woebbecke et al. 1995, Toomey et al. 2015) and is simply the chromatic coordinate of the green channel expressed as a proportion of the sum of coordinates, which eliminates the influence of illumination on green brightness and is given by:

$$GCC = \frac{G}{R+G+B} \quad \text{[eq. 2]}$$

* The green red vegetation index was first used by Rouse et al. (1973 & 1974) who concluded it could be used for several measures of crops and rangelands. Their conclusions have been later confirmed in several occasions (Tucker 1978; Falkowski et al. 2005, Motohka et al. 2010, Viña et al. 2011). This index is given by:

$$GRVI = \frac{G-R}{G+R} \quad \text{[eq. 3]}$$

* Lastly, the visible atmospherically resistant index (VARI) was proposed by Gitelson et al. (2002) in order to correct GRVI for atmospheric effects and was found to show a higher relation with vegetation fraction that its uncorrected counterpart. It is defined as:

$$VARI = \frac{G-R}{G+R-B} \quad \text{[eq. 4]}$$

We calculated all four greenness indices directly from their digital numbers as provided by the jpg format the camera stores the images with, instead of calculating reflectance values. As we were not using reflectance for calculating these indices their properties might not be the same as described by other authors (Tucker 1978, Gitelson et al. 2002, Motohka et al. 2010). Still, we expected them to be useful in our context and decided to use this simpler approach, as our aim was to get as simple a workflow as possible in order to allow for an easy, handy use of UAV imagery by non-expert users.

Index calculations and their posterior analysis were carried out in QGIS, by combining the use of raster calculator with specific tools of zone statistics and spatial joining. The whole process for each index, after its calculation, involved the following steps:

- Applying the greenness threshold to the indices layers, in order to erase all non-green pixels, which were set to 0. We selected as green pixels those where the green channel showed higher digital numbers than the channels it was compared to. For ExGI, GRVI and VARI, hence, we selected those pixels with values greater than 0 as green pixels, and reclassified values less than 0 as 0. For GCC, the applied threshold was 1/3, and hence all values equal to or lesser than were set to 0.
- Calculating the zone statistics of the greenness index and the filtered canopy height model for each 5*5-m2 cell within the study area. Zone statistics produces six different measures of the index value per each cell: count, mean, standard deviation, median, maximum and minimum.
- Calculating the pooled DBH of all measured pines within the cells of this same grid.

2.3. Statistical analysis

We aimed to assessthe recovery of pines in the areas burnt in 1998. Hence, we selected the sum of the diameter at the breast height (DBH) of all pines within a cell as our response variable. DBH was highly correlated to pine height (see Supplementary Material S1) and its measure in pines is easier and less prone to measurement errors. DBH has also been related to many other morphological

and functional traits (Ribbens et al. 1994, Parresol 1999, Bolte et al. 2004, Poorter et al. 2006, 2008, He et al. 2018) and hence it is open to a more insightful analysis.

First, we carried out simple linear regression analysis of the sum of DBH on the four greenness indices and on the canopy height model. For each greenness index and the canopy height model, we fitted 6 models, where the derived explanatory variables corresponded to seven different summary statistics per 5 m grid-cell: count of points with non-zero values for the corresponding index or canopy height model and sum, mean, standard deviation, maximum and median of the values of all points within the cell. Our aim was to explore which statistic could be better suited for its use in total DBH estimation from greenness index maps and canopy height models. Then we tried to improve model fit by combining greenness indices with pine canopy height, by means of multiple linear regression analysis.

R2 (for simple linear models) and adjusted R2 (for multiple linear models) and scatterplots were used throughout to assess model fit and comparing models.

All statistics were carried out in R (R Core Team 2016), by means of the R-Studio integrated development environment (RStudio Team, 2015).

3. Results

Two pine species were found in both study sites, black pine (Pinus nigra) and Scots pine (Pinus sylvestris), although only one individual of the latter was recorded in La Carral site. Mean tree height was 124.94 cm (s.d.= 88.78) for black pine and 188,15 (s.d.=117.87) for Scotch pine in Cal Rovira-Sanca and 109.82 (sd=51.38) for black pine in La Carral, while the only Scotch pine in this site was 230 cm high. DBH values were lower for black pine than for Scotch pine, around 3.25 cm (mean=3.36 and s.d.=2.1 for Cal Rovira-Sanca; mean = 3.2 and s.d.=1.87 for La Carral) versus 5 (mean=4.91 and s.d.=3.12 in Cal Rovira-Sanca 6.6 cm for the only tree in La Carral).

The proportion of small trees was high for both species, but higher for black pine: median height of 117.5 and 105 and median DBH of 3.1 and 2.4 for Cal Rovira-Sanca and La Carral, respectively, as opposed to a median height of 192,5 and median DBH of 4.1 in Cal Rovira-Sanca for the Scotch pine (see Supplementary Material S1).

3.1. Greenness indices

Greenness indices showed to be much better proxies for the sum of pine DBH than for canopy height in both La Carral and Cal Rovira-Sanca. In fact, mean R2 for the regressions of sum of pine DBH on the different statistics of greenness indices values ranged between 0.005 and 0.466, while the regressions of the sum of pine DBH on canopy statistics ranged from 0.008 to 0.028 (table 1; figure 3). However, large differences were found among greenness indices. Even if GRVI and VARI still resulted in higher R2 than any pine canopy height model, they were clearly outperformed by ExGI and GCC, which reached a maximum R2 of more than 45% (table 1).

Different statistics for the four greenness indices showed markedly differing fits on the sum of pine DBH, as shown by the high coefficients of variation of R2 (table 1; figure 3). There were not clear-cut patterns of precision among the tested statistics that can be considered general for all four indices, although the count of non-zero values appears as the most consistently unreliable measure, with CVs higher than 100% for the all four indices.

Table 1. Summary statistics of the determination index (R2) for the simple regressions of the sum of pine DBH on the four greenness indices and the canopy height model. Figures show the average R2 across flights (two sites at each of two flight altitudes) and its coefficient of variation, expressed as percentage (within brackets). CHM stands for canopy height model. See "Imagery analysis" for a definition of the four indices.

	ExGI	GRVI	GCC	VARI	All Indices	CHM
Count of non zero index	0,154 (124,0)	0,114 (118,4)	0,147 (127,9)	0,121 (119,8)	0,134 (14,5)	0,028 (50,0)
Max index value	0,389 (27,2)	0,164 (98,2)	0,297 (37,7)	0,051 (119,6)	0,225 (65,9)	0,014 (121,4)
Mean index value	0,401 (12,7)	0,195 (61,0)	0,370 (50,5)	0,039 (184,6)	0,251 (66,9)	0,015 (113,3)
Median index value	0,227 (80,6)	0,162 (50,6)	0,182 (103,3)	0,076 (118,4)	0,162 (39,1)	0,008 (125,0)
Std index values	0,440 (37,3)	0,152 (57,9)	0,466 (32,2)	0,005 (40,0)	0,266 (84,5)	0,018 (100,0)
Sum of index values	0,256 (40,2)	0,088 (78,4)	0,155 (122,6)	0,027 (122,2)	0,132 (74,6)	0,014 (114,3)
All measures	0,311 (36,8)	0,146 (26,4)	0,270 (48,4)	0,053 (76,8)		0,016 (41,1)

3.2. Canopy height

A Canopy height alone shows a very poor explanatory power of the sum of DBH of pines, with a pooled mean of R2 of 0,016, well below the values obtained from the four greenness indices. Accordingly, jointly considering greenness indices and canopy height does not increase adjusted R2 more than 10% (figure 3). For both sites and both flight heights, however, the best fitting model included always a canopy height statistics (figure 4).

Different statistics of the canopy height model resulted in markedly different models (table 1), with adjusted R^2s varying between 0.8 and 28%. The canopy statistics that provided the highest R2 for the regression on the sum of pine DBH was the count of cells with non-zero values, although it was not the one producing the best models when combined with greenness indices (table S1).

3.3. Flight altitude

The altitude of the flight did not severely affect the capacity to estimate the sum of pine DBH per grid-cell (figures 3 and 4). However, the best fits were always achieved for 100 m flights (figure 3), although with a larger difference in Cal Rovira-Sanca.

Figure 3. Values of the determination coefficient from the OLS regressions of the four greenness indices on the sum of DBH. Upper panel: simple regressions. Lower panel: multiple regressions where canopy height statisticsincluded as additionalexplanatory variables.

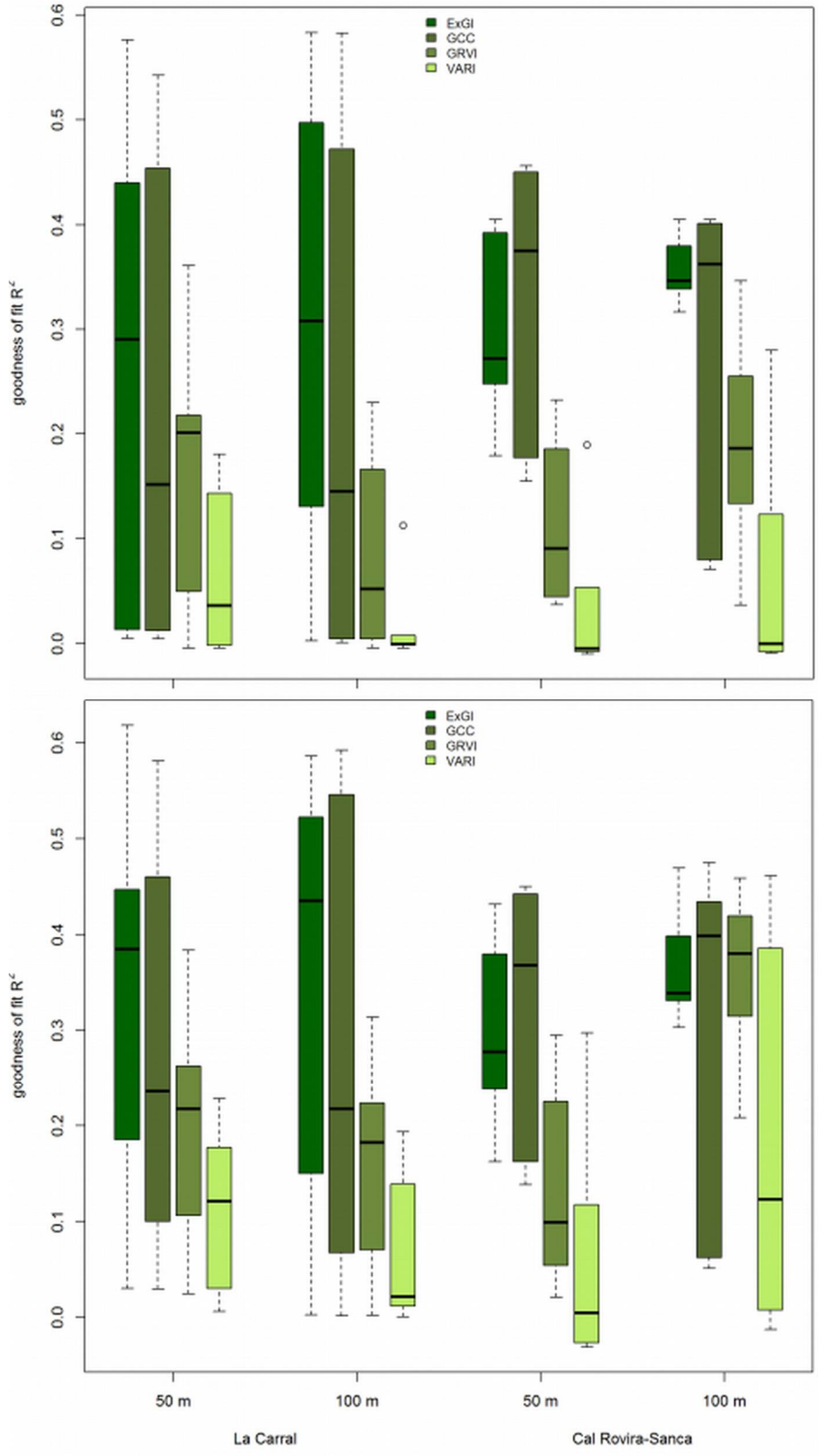

277

278 **Figura 4**. 3D scatterplots showing the best fitting model as assessed per site and flight altitude. All
279 variables correspond to summary statistics within each 5*5 m cell (see text for details).

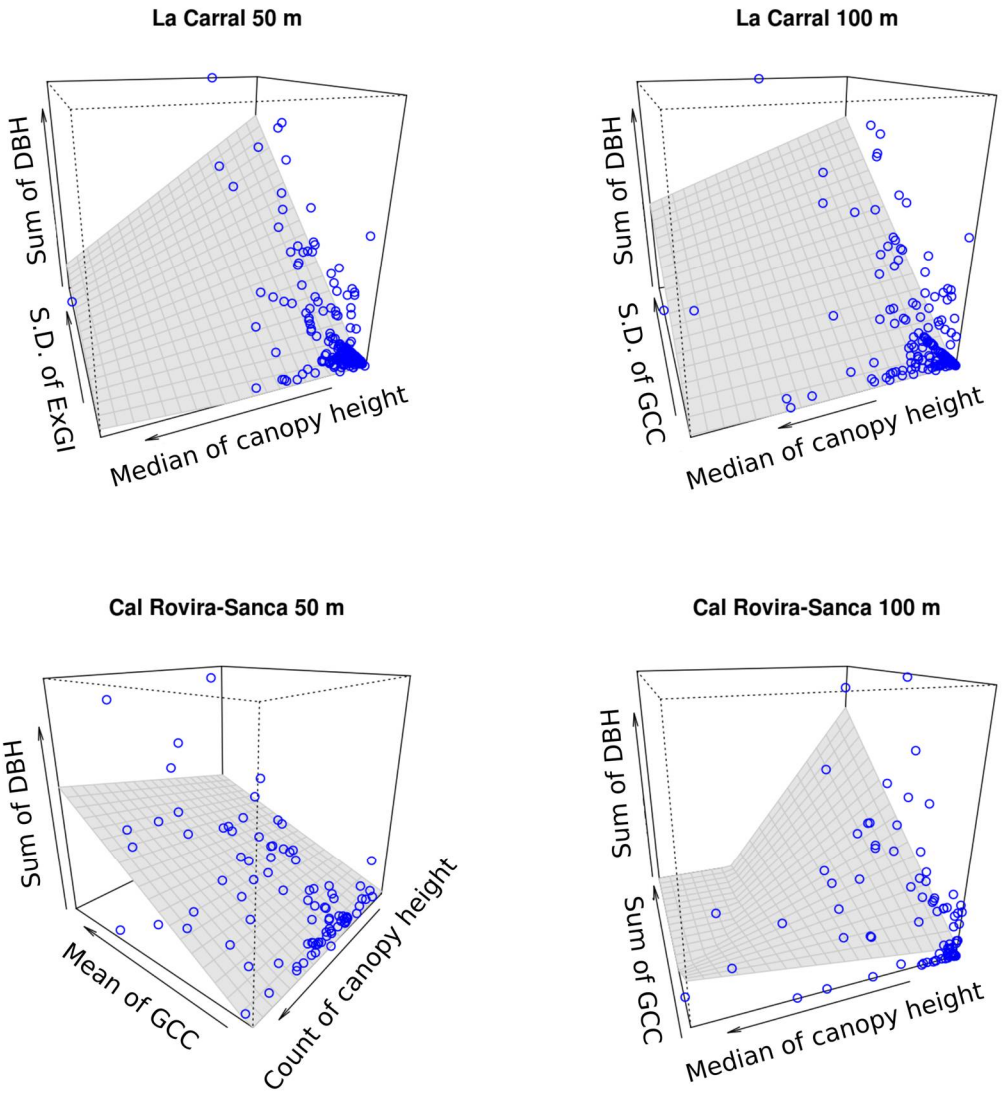

3.4. Global- and flight-wise best models

Overall, the model with a best fit was that including the standard deviation of the GCC index and the median of the canopy height model. It generally achieves fits close to those of the best fitting model for each of the flights (figures 4 and S5-1, tables S3), although the difference was higher for the 50 m flight in Cal Rovira-Sanca.

4. Discussion

We have used a simple and low cost UAV to monitor pine regeneration after fire in a regenerating forest growing on rocky substrates. We have further analyzed the effect of flight altitude on model performance and compared the efficiency of different greenness indices or visual vegetation indices. Two different sites were flown with the UAV at altitudes of 50 m and 100 m and the resulting orthoimage and digital surface model were analyzed to calculate a canopy height model and four different greenness indices: excess green index (ExGI), green color coordinate (GCC), green-red vegetation index (GRVI) and visible atmospherically resistant index (VARI). The measured obtained were finally statistically related to direct measures taken in the field.

Our results show that low cost UAV platforms are a useful alternative to professional platforms when it comes to the detailed, cost-effective monitoring of forest ecosystems and forest recovery after

disturbance, especially in non-profit forests where economic and human resources may be scarcer. By using a simple approach with a consumer level UAV platform and low cost or free software, we have predicted post fire pine cover recovery (estimated as the sum of pine DBH)with a relatively high coefficient of determination of up to 60%. Furthermore, the application of all the software used has been performed on d, with no tweaking of any of their characteristics. This allows the use of this kind of procedures to end users, working in forestry and applied research, and at the same time leaves margin for further improving the accuracy of the process.

UAVs are being increasingly use in ecological and conservation studies and monitoring, due to their multiple advantages, such as an increased spatial resolution, lower cost and higher acquisition flexibility (Hardin & Hardin 2010, Colomina & Molina 2014), which also allows a higher temporal resolution. Low cost models increase flexibility of use and general costs, as compared to professional platforms, and at the same time reduce considerably their learning slope, which has been deemed too steep (). Yet, despite their low cost and ease of use, they accomplish spatial resolution way higher than those of aerial orthoimagery and provide useful results with a limited effort in image post-processing and analysis. This cost reduction is especially important for ecological studies and monitoring in non-profit forests and other habitats. In fact, nowadays, close forests make up only a small fraction of the experiments with UAVs in the field, while high value crops and forests are the main focus of most of them (Salamí et al. 2014).

The flexibility and low cost of UAV deployment have been key factors determining the results of our pine estimation, as it allowed flying during the end of winter, before Portuguese oaks shed their leaves and the grass becomes growing after the winter. This strategy of seeking the best moment to maximize spectral difference among habitat components is paramount when it comes to discriminating different plant species or vegetation types from visual spectrum cameras and has previously used (Leduc & Knudby 2018).

Since the proposal of the first two vegetation indices by Pearson and Miller (1972), and that of the NDVI shortly after by Rouse et al. (1973), a high number of vegetation indices have been proposed and used for the study of vegetation from satelite, airplane and UAV sensor imagery (see for example Bannari et al. 1995, Gitelson et al. 2002, Viña et al. 2011, Baluja et al. 2012, Sonnentag et al. 2012). Most of them rely on the use of near infrared region (NIR), which profits from the marked difference in the absorbance spectrum of chlorophyll between red and near infrared regions. The use and development of those indices that rely exclusively on the visual spectrum has sharply increased during last years, though, as a way to overcome the limited choice of spectrum bands in most UAV carried sensors. Assessment of their differential performance has yielded unconclusive results (Tucker 1978, Woebbecke et al. 1995, Gitelson et al. 2002, Falkowski et al. 2005, Sonnentag et al. 2012, Motohka et al. 2010, Toomey et al. 2015), but may even be better than those that include a NIR band (Falkowski et al. 2005, Rasmussen et al. 2016). Our results match those of Woebbecke et al. (1995) who reported ExGI and GCC to perform better than other four indices when discriminating vegetation from nonplant background in different light conditions. Sonnentag et al. (2012) recommended using GCC over ExGI to examine vegetation phenology in repeat photography studies, due to its lower sensitivity to changes in scene illumination. In our two sites, GCC also achieved higher accuracies when estimating pine cover in regenerating forests than ExGI.

By combining these indices with information derived from a canopy height model, we obtained determination coefficients for the pooled DBH of pines of up to 60%. These figures are comparable to those reported in similar studies with agricultural plots relating vegetation indices with vegetation fraction or cover (Geipel et al. 2014, Díaz-Varela et al. 2015, Rasmussen et al. 2016), as well as in forest studies with (Puliti et al. 2015, Modzelewska et al. 2017). For example, Puliti et al. (2015) achieved a 60% determination coefficient when estimating basal area from UAV imagery, by combining point density and height. In our case, the canopy height model only improved the fit slightly (around 10%), probably due to the small size of most of the pines in both of our study sites. Later stages in the regeneration of vegetation would probably change the role of canopy height models in pine abundance prediction, as they would allow to better discriminate pines from tall grasses and shrubs.

Trials with canopy height of green pixels did not improve the fit of our models in this early stage (unpublished data).

We did not find marked differences between two contrasting flight altitudes in the general performance of greenness indices, although the selection of optimal greenness index or cell statistic depended on altitude at both sites. Flight altitude was an important determinant of the estimate of vegetation cover of wheat and barley experimental crops, together with growth stage and stitching software (Rasmussen et al. 2016). Flight altitude determines the final image resolution obtained as well as the effect of topography on radiance (by changing the relative angle between terrain slopes and the UAV), and hence, values of greenness indices (Burkart et al. 2015, Rasmussen et al. 2016). Although a change of scale can be expected to modify the determination coefficient of greenness indices, by changing the greenness values of each pixel (Mesas-Carrascosa et al. 2015), we did not notice any remarkable effect, probably because our analysis relied on descriptive statistics encapsulating information at a coarser spatial extent of 5*5 m (figure S5). Topography was not expected to introduce important variations on the values of greenness indices, as the topography of our field plots was relatively mild and homogeneous.

The UAV deployment and imagery analysis we present here has its own limitations leading to areas for further improvement of image acquisition and analysis. First, the camera used has a FOV of 120º and non-rectilinear lenses, which results in a heavy fish-eye effect. Although the processing of images within Agisoft Photoscan corrects for lens distortion before carrying out the image matching process, the effect of distortion on image quality is too high beyond 50 m of the image center and may result in a low quality in important fractions of the orthoimage. However, quality of low cost UAVs has rapidly increased parallel to the decrease in their relative price.

Second, trying to reduce complexity of deployment and analysis to a minimum, we did not place ground control points and so, spatial accuracy of the obtained orthoimage was limited by the resolution of the PNOA imagery (pixel size of 25 cm and RMSE below 50 cm). Although most present day low cost UAVs geotag the images taken on the fly, their GPS accuracy is still low and commonly results in location errors of few meters. Hence, if we aim to reduce costs to a minimum , we are to deploy several ground control points around the plot to increase the spatial accuracy. The spatial accuracy we get when using GCPs will ultimately depend on the accuracy of GCP location measurement, which may be reduced to centimeters or even millimeters with differential (DGPS) or RTK GPS measurements.

The camera we used is recording data only on the visual spectrum. While this is one of the strengths of our work (due to its availability and ease of operation), it also limits the capacity to properly discriminate the photosynthetically active vegetation from the dormant vegetation. Capturing near infrared radiation (NIR) requires a more expensive, multispectral, These kind of multispectral cameras are more readily available for UAVs deployment and the assessment of its value in forestry is under current development and will prove specially suitable for multitemporal image acquisition and comparison (Nebiker et al. 2008, del Pozo et al. 2014, Suomalainen et al. 2014).

All in all, consumer level UAVs can be expected to provide a common low cost tool for ecological monitoring of after fire recovery and other conservation and monitoring tasks, with increasingly lower prices, higher accuracy levels and wider application types.

Supplementary Materials: The following are available online at www.mdpi.com/xxx/s1, Figure S1.1. Height distribution of Pinus nigra and Pinus sylvestris in La Carral and Cal Rovira-Sanca, as measured in the field, Figure S1.2. Diameter at breast height (DBH) distribution of Pinus nigra and Pinus sylvestris in La Carral and Cal Rovira-Sanca, as measured in the field, Figure S1.3. Regressions of tree height on DBH for both species in La Carral and Cal Rovira-Sanca, Figure S2-1. General workflow followed for the anlaysis of UAV imagery and the software frameworks used in each of the steps. Numbers refer to the different intermediate outputs shown in figure S2, Table S3-1. Estimates of the best fitting model for the 50 m high flight in La Carral, with one greenness index (ExGI) and one pine canopy height model (GCC CAN), Table S3-2. Estimates of the best fitting model for the 100 m high flight in La Carral, with one greenness index (GCC) and one pine canopy height model (GCC CAN), Table S3-3. Estimates of the best fitting model for the 50 m high flight in Cal Rovira-Sanca, with one greenness index (GCC) and one pine canopy height model (ExGI CAN), Table S3-4. Estimates of the best fitting model for the 50 m high flight in Cal Rovira-Sanca, with one greenness index (GCC) and one pine canopy height

model (ExGI CAN), Figure S4-1. Maps of the four greenness indices and the estimated canopy model from the four flights carried out at two sites and two flight altitude. Colors have been differentially scaled for the four greenness indices and four flights, due to different value ranges, while the color scale is common for the four canopy height models (CHM), Figure S5-1. 3D scatterplots showing the overall best fitting model applied to each site and flight altitude.

Author Contributions: Conceptualization, A.R.L. and L.B.; methodology, A.R.L. and L.B.; software, A.R.L.; validation, A.R.L. and L.B.; formal analysis, A.R.L.; investigation, A.R.L. and L.B.; resources, L.B; data curation, A.R.L.; writing—original draft preparation, A.R.L.; writing—review and editing, A.R.L. and L.B.; visualization, A.R.L.; supervision, L.B.; project administration, L.B.; funding acquisition, L.B.

Funding: ARL benefited from the support of the NEWFOREST Marie Curie IRSES project.

Acknowledgments: We are indebted to Jan and Martí Brotons for their collaboration on field measurements.

Conflicts of Interest: "The authors declare no conflict of interest."

References

1. AgiSoft PhotoScan Professional (Version 1.2.6) [Software] 2016. Retrieved from http://www.agisoft.com/downloads/installer/
2. Baena, S.; Moat, J.; Whaley, O.; Boyd, D. S. 2017 Identifying species from the air: UAVs and the very high resolution challenge for plant conservation. PLoS ONE 12(11): e0188714. https://doi.org/10.1371/journal.pone.0188714.
3. Baluja, J.; Diago, M. P.; Balda, P.; Zorer, R.; Meggio, F.; Morales, F.; Tardaguila, J. 2012 Assessment of vineyard water status variability by thermal and multispectral imagery using an unmanned aerial vehicle (UAV). Irrig. Sci.: 30: 511-522.
4. Blaschke, T. 2010 Object based image analysis for remote sensing. ISPRS J Photogram. Remote Sens., 65: 2-16.
5. Bolte, A.; Rahmann, R.; Kuhr, M.; Pogoda, P.; Murach, D.; Gadow, K. v. 2004 Relationships between tree dimension and coarse root biomass in mixed stands of European beech (Fagus sylvatica L.) and Norway spruce (Picea abies [L.] Karst.). Plant and Soil 264: 1-11.
6. Burkart, A.; Aasen, H.; Alonso, L.; Menz, G.; Bareth, G.; Rascher, U. 2015 Angular dependency of hyperspectral measurement over wheat characterized by a novel UAV based goniometer. Remote Sens. 6: 725-746.
7. Chehata, N.; Orny, C.; Boukir, S.; Guyon; D. 2011 Object-based forest change detection using high resolution satellite images. In: Stilla, U. et al. (eds.) PIA11. International Archives of Photogrammetry, Remote Sensing and Spatial Information Sciences, 38: 3/W22.
8. CloudCompare 2.7.0. [GPL software] 2016 Retrieved from http://www.cloudcompare.org/.
9. Colomina, I.; Molina, P. 2014 Unmanned aerial systems for photgrammetry and remote sensing: A review. ISPRS Journal of Photogrammetry and Remote Sensing 92: 79-97.
10. del Pozo, S.; Rodríguez-Gonzálvez, P.; Hernández-López, D.; Felipe-García, B. 2014 Vicarious radiometric calibration of a multispectral camera on board an unmanned aerial system. Remote Sens. 6: 1918-1937.
11. Díaz-Varela, R.; de la Rosa, R.; León, L. e Zarco-Tejada, P. J. 2015 High-resolution airborne UAV imagery to assess olive tree crown parameters using 3D photo reconstruction: application in breeding trials. Remote Sens. 7: 4213-4232.

12. Falkowski, M. J.; Gessler, P. E.; Morgan, P.; Hudak, A. T.; Smith; A. M. S. 2005 Characterizing and mapping forest fire fuels using ASTER imagery and gradient modeling. Forest Ecology and Management, 217: 129-146.
13. Geipel, J.; Link, J.; Claupein, W. 2014 Combined spectral and spatial modelling of corn yield based on aerial images and crop surface models acquired with an unmanned aircraft system. Remote Sens. 11: 10335-10355.
14. Getzin, S.; Nuske, R. S. e Wiegand, K. 2014 Using unmenned aerial vehicles (UAV) to quantify spatial gap patterns in forests. Remote Sens. 6: 6988-7004.
15. Gianetti, G.; Chirici, G.; Gobakkern, T.; Næsset, E.; Travaglini, D.; Puliti, S. 2018 A new approach with DTM-independent metrics for forest growing stock prediction using UAV photogrammetric data. Remote Sensing of Environment 213: 195-205.
16. Gitelson, A. A.; Kaufman, Y. J.; Stark, R.; Rundquist, D. 2002 Novel algorithms for remote estimation of vegetation fraction. Remote Sensing of Environment, 80: 76.87.
17. XnView MP 0.83 [GPL software] 2016 Retrieved from https://www.xnview.com/en/xnviewmp/.
18. Guerra-Hernández, J.; González-Ferreiro, E.; Sarmento, A.; Silva, J.; Nunes, A.; Correia, A. C.; Fontes, L; Tomé, M. e Díaz-Varela, R. 2016 Using high resolution UAV imagery to estimate tree variables in Pinus pinea plantation in Portugal. Forest Systems 25(2): 2171-9845.
19. Hardin, P. J.; Hardin, T. J. 2010 Small-scale remotely piloted vehicles in environmental research. Geography Compass 4/9: 1297-1311.
20. Harriman, L.; Muhlhausen, J. 2014 A new eye in the sky: Eco-drones. In: UNEP Emerging Environmental Issues 2013, Division of Early Warning and Assessment, UNEP, Nairobi. pp: 47-55.
21. He, H.; Zhang, C.; Zhao, X.; Fousseni, F.; Wang, J.; Dai, H.; Yang, S.; Zuo, Q. 2018 Allometric biomass equations for 12 tree species in coniferous and broadleaved mixed forests, Northeastern China. PloS ONE 13: e0186226. URL: https://doi.org//10.1371/journal.pone.0186226
22. Institut Cartogràfic i Geològic de Catalunya 2014 Mapa geològic amb llegenda interactiva (versió 2). URL: http://betaportal.icgc.cat/wordpress/mapa-geologic-amb-llegenda-interactiva/. Accessed: 2017-13-01.
23. Karpina, M.; Jarząbek-Rychard, M.; Tymków, P.; Borkowski, A. 2016 UAV-based automatic tree growth measurement for biomass estimation. The International Archives of the Photogrammetry, Remote Sensing and Spatial Information Sciences, Volume XLI-G8, XXIII ISPRS Congress, 12-19 July 2016, Prague, Czech Republic.
24. Leduc, M.-B.; Knudby, A. J. 2018 Mapping wild leek through the forest canopy using a UAV. Remote Sensing 10(1): 70; https://doi.org/10.3390/rs10010070.
25. Matese, A.; Toscano, P.; Di Gennaro, S. F.; Genesio, L.; Vaccari, F. P.; Primicerio, J.; Belli, C.; Zaldei, A.; Bianconi, R.; Gioli, B. 2015 Intercomparison of UAV, aircraft and satellite remote sensing platforms for precision viticulture. Remote Sensing 7: 2971-2990.
26. McGaughey, R. J. 2016 Fusion/LDV: Software for Lidar Data Analysis and Visualization. October 2016 – Fusion Version 3.60. US Department of Agriculture, Forest Service, Pacific Northwest Research Station: Seattle, WA, USA.
27. Mesas-Carrascosa, F.-J.; Torres-Sánchez, J.; Clavero-Rumbao, I.; García-Ferrer, A.; Peña, J.-M.; Borra-Serrano, I.; López-Granados, F. 2015 Assessing optimal flight

parameters for generating accurate multispectral orthomosaics by UAV to support site-specific crop management. Remote Sensing 7: 12793-12814.

28. Modzelewska, A.; Stereńczak, K.; Mierczyk, M.; Maciuk, S.; Balazy, R.; Zawila-Niedźwiecki, T. 2017 Sensitivity of vegetation indices in relation to parameters of Norway spruce stands. Folia Forestalia Polonica, series A – Forestry, 59: 85-98.
29. Motohka, T.; Nasahara, K. N.; Oguma, H.; Tsuchida, S. 2010 Applicability of green-red vegetation index for remote sensing of vegetation phenology. Remote Sensing 2: 2369-2387.
30. Nebiker, S.; Annen, A.; Scherrer, M.; Oesch, D. 2008 A light-weight multispectral sensor for micro UAV-opportunities for very high resolution airborne remote sensing. The International Archives of the Photogrammetry, Remote Sensing and Spatial Information Sciences, Vol XXXV, Part B1. Beijing.
31. Parresol, B. R. 1999 Assessing tree and stand biomass: a review with examples and critical comparisons. Forest Sci. 45:573 - 593.
32. Poorter, L.; Bongers, L.; Bongers, F. 2006 Architecture of 54 moist-forest tree species: traits, trade-offs, and functional groups. Ecology, 87: 1289-1301.
33. Poorter, L.; Wright, S. J.; Paz, H.; Ackerly, D. D.; Condit, R.; Ibarra-Manríquez, G.; Harms, K. E.; Licona, J. C.; Martínez-Ramos, M.; Mazer, S. J.; Muller-Landau, H. C.; Peña-Claros, M.; Webb, C. O.; Wright, I. J. 2008 Are functional traits good predictors of demographic rates? Evidence from five neotropical forests. Ecology, 89: 1908-1920.
34. Puliti, S.; Ørka, H. O.; Gobakken, T.; Næsset, E. 2015 Inventory of small forest areas using and unmanned aerial system. Remote Sens. 7: 9632-9654.
35. Puliti, S., 2018 Tree-stump detection, segmentation, classification, and measurement using unmanned aerial vehicle (UAV) imagery. Forests, 9: 102. doi: 10.3390/f9030102.
36. Rasmussen, J.; Ntakos, G.; Nielsen, J.; Svensgaard, J.; Poulsen, R. N. and Christensen, S. 2017 Are vegetation indices derived from consumer-grade cameras mounted on UAVs sufficiently reliable for assessing experimental plots? Europ. J. Agronomy 74: 75-92.
37. R Core Team 2016 R: A language and environment for statistical computing. R Foundation for Statistical Computing, Vienna, Austria. URL: https://www.R-project.org/.
38. Ribbens, E.; Silander, Jr., J. A.; Pacala, S. W. 1994 Seedling recruitment in forests: calibrating models to predict patterns of tree seedling dispersion. Ecology, 75: 1794-1806.
39. Rodrigo, A.; Retana, J.; Picó, X. 2004 Direct regeneration is not the only response of Mediterranean forests to large fires. Ecology 85: 716-729.
40. RStudio Team 2015 RStudio: Integrated Development for R. RStudio, Inc., Boston, MA URL http://www.rstudio.com/.
41. Salamí, E.; Barrado, C.; Pastor, E. 2014 UAV fligh experiments applied to the remote sensing of vegetated areas. Remote Sens 6: 11051-11081.
42. Sonnentag, O.; Hufkens, K.; Teshera-Sterne, C.; Young, A. M.; Friedl, M.; Braswell, B. H.; Milliman, T.; O'Keefe, J.; Richardson, A. D. 2012 Digital repeat photography for phenological research in forest ecosystems. Agricultural and Forest Meteorology 152: 159-177.

43. Suomalainen, J.; Anders, N.; Iqbal, S.; Roerink, G.; Franke, J.; Wenting, P.; Hünniger, D.; Bartholomeus, H.; Becker, R.; Kooistra, L. 2014. A lightweight hyperspectral mapping system and photogrammetric processing chain for unmanned aerial vehicles. Remote Sens., 6: 11013-11030.

44. Thiel, C.; Schmullius, C. 2017 Comparison of UAV photograph-based and airborne lidar-based point clouds over forest from a forestry application perspective. Internation Journal of Remote Sensing, 38: 2411-2426.

45. Toomey, M.; Friedl, M. A.; Frolking, S.; Hufkens, K.; Klosterman, S.; Sonnentag, O.; Baldocchi, D. D.; Bernacchi, C. J.; Biraud, S. C.; Bohrer, G.; Brzostek, E.; Burns, S. P.; Coursolle, C.; Hollinger, D. Y.; Margolis, H. A.; McCaughey, H.; Monson, R. K.; Munger, J. W.; Pallady, S.; Phillips, R. P.; Torn, M. S.; Wharton, S.; Zeri, M.; Richardson, A. D. 2015 Greenness indices from digital cameras predict the timing and seasonal dynamics of canopy-scale photosynthesis. Ecological Applications 25(1): 99-115.

46. Torres-Sánchez, J.; López-Granados, F.; Serrano, N.; Arquero, O.; Peña, J. M. 2015 High-trhoughput 3-D monitoring agricultural-tree plantations with unmanned aerial vehicle (UAV) technology. PloS ONE, 10(6): e0130479. Doi: 10.1371/journal.pone.0130479.

47. Tucker, C. J. Red and photographic infrared linear combinations for monitoring vegetation. NASA Technical Memorandum 79620. NASA, Maryland. 37 pp.

48. Viña, A.; Gitelson, A. A.; Nguy-Robertson, A. L.; Peng, Y. 2011 Comparison of different vegetation indices for the remote assessment of green leaf area index of crops. Remote Sensing of Environment 115: 3468-3478.

49. Wallace, L.; Lucieer, A.; Watson, C.; Turner, D. 2012 Development of a UAV-LiDAR system with application to forest inventory. Remote Sens. 4: 1519-1543.

50. Wallace, L.; Lucieer, A.; Malenobský, Z.; Turner, D.; Vopěnka, P. 2016 Assessment of forest structure using two UAV techniques: a comparison of airborne laser scanning and structure from motion (SfM) point clouds. Forests, 7:62. Doi: 10.3390/f7030062.

51. Westoby, M. J.; Brasington, J.; Glasser, N. F.; Hambrey, M. J.; Reynolds, J. M. 2012 'Structure-from-Motion' photgrammetry: a low-cost, effective tool for geoscience applications. Geomorphology, 179: 300-314.

52. Woebbecke, D. M.; Meyer, G. E.; Von Bargen, K.; Mortensen, D. A. 1995 Color indices for weed identification under various soil, residue, and lighting conditions. Transactions of the American Society of Agricultural Engineers, 38(1): 259-269.